# Exploration of Energy Storage Materials for Water Desalination via Next-Generation Capacitive Deionization

*Wenhui Shi[1†], Xinlong Gao[2†], Jing Mao[2], Xin Qian[1], Wenxian Liu[2], Fangfang Wu[2], Haibo Li[3*], Zhiyuan Zeng[4*], Jiangnan Shen[1*] and Xiehong Cao[2*]*

[1] Center for Membrane Separation and Water Science & Technology, Ocean College, Zhejiang University of Technology, Hangzhou, China, [2] College of Materials Science and Engineering, Zhejiang University of Technology, Hangzhou, China, [3] Ningxia Key Lab Photovolta Material, Ningxia University, Yinchuan, China, [4] Department of Materials Science and Engineering, City University of Hong Kong, Hong Kong, China

Clean energy and environmental protection are critical to the sustainable development of human society. The numerous emerged electrode materials for energy storage devices offer opportunities for the development of capacitive deionization (CDI), which is considered as a promising water treatment technology with advantages of low cost, high energy efficiency, and wide application. Conventional CDI based on porous carbon electrode has low salt removal capacity which limits its application in high salinity brine. Recently, the faradaic electrode materials inspired by the researches of sodium-batteries appear to be attractive candidates for next-generation CDI which capture ions by the intercalation or redox reactions in the bulk of electrode. In this mini review, we summarize the recent advances in the development of various faradaic materials as CDI electrodes with the discussion of possible strategies to address the problems present.

**Keywords: energy storage, sodium-ion battery, capacitive deionization, water desalination, faradaic electrode**

## INTRODUCTION

Clean energy and environmental protection are critical to the sustainable development of human society (Panwar et al., 2011; Shahzad et al., 2017; Liu et al., 2019a). Over the past decades, great efforts have been devoted to the development of various electrochemical energy storage devices, such as lithium-ion batteries sodium-ion batteries (SIBs) (Zhang et al., 2018; Zubi et al., 2018), SIBs (Chao et al., 2018; Delmas, 2018; Fang et al., 2018), metal-air batteries (Zhang X. et al., 2016), and supercapacitors (Raza et al., 2018; Xu et al., 2018; Han Y. et al., 2019). On the other hand, water desalination has played an essential role in resolving the water crisis. Compared with other existing desalination technologies, capacitive deionization (CDI) has the key advantages of low cost, high energy efficiency, easy regeneration, and wide application (Suss et al., 2015). Beyond the desalination of brackish water, CDI has been also applied in wastewater remediation (Wang Z. J. et al., 2017), water softening (Wang and Lin, 2019), the removal of heavy metals (Huang et al., 2016) and organic pollutants (Bharath et al., 2017), as well as ion separation (Shi et al., 2019a).

The concept of CDI was reported as early as 1960s, but the term of CDI was proposed by Farmer et al. until 1996 (Farmer et al., 1996). In recent decades, the research interests in CDI have exponentially grown with the advances of novel electrode materials, cell configurations, and better understanding of ion electrosorption behaviors (Oladunni et al., 2018; Tang et al., 2019). CDI has

many similarities with electrochemical energy storage systems, especially supercapacitors, sodium ion batteries (Kim et al., 2014; Fang et al., 2019), etc. These two fields can find common ground in related researches, such as the design of electrode materials, interfacial electrochemistry, and the ion diffusion process in micro-/nano-structured materials (Shi et al., 2019c).

As shown in **Figure 1A**, CDI cells are typically composed of two parallel porous electrodes with a channel in between for water flow. The most widely used electrode for traditional CDI is carbon materials. When a voltage difference of generally ~1 V is applied across the CDI cell, ions are capacitively stored in the porous electrode by forming electrical double layers (EDLs), thereby removing the salt ions from the feed water. When the external power supply is removed or the polarity is reversed, the electrode can be regenerated with the adsorbed ions released to the brine. It is worth mentioning that recently some newly developed configurations of CDI cells have adopted faradaic electrode materials used in batteries, such as hybrid CDI (Lee et al., 2014). Differing from carbon electrodes, faradaic materials store ions by intercalation or redox reactions (inset in **Figure 1A**) (Pasta et al., 2012). The desalination/regeneration process of CDI is very similar to the charge/discharge process of energy storage devices (**Figure 1B**). In this mini review, we briefly introduce the key features of CDI and aqueous electrochemical energy storage devices in common, in terms of principle and design strategy of electrode materials. In particular, possible strategies and emerging trends to address the challenges present in CDI were discussed. This review may provide a new insight to the development of novel faradaic electrode materials for the next-generation CDI system.

# CARBON MATERIALS

CDI shares a lot of electrode materials with electrochemical energy storage devices. The CDI and energy storage performances of the representative electrode materials are summarized in **Table 1**. Among these materials, carbonaceous materials have been widely used in electrochemical sodium storage devices, such as SIBs and sodium ion capacitors (Balogun et al., 2016). They are also the most commonly explored electrodes for conventional CDI, which is based on the EDLs effect of carbon materials to capture ions from salty water (Noonan et al., 2018). Carbon electrode-based CDI has a desalination capacity of about 0.7–14.3 mg g$^{-1}$ (Porada et al., 2013). Recently developed nano-carbon electrodes, such as graphene (Xu et al., 2015a; Zhang et al., 2019), carbon with functional groups (Gao et al., 2016), and hierarchical carbon materials (Gao et al., 2015), can increase the desalination capacity up to 57.13 mg g$^{-1}$ (Li et al., 2017).

CDI performance of graphene was first reported by Li et al. showing a relatively low desalination capacity of 4.29 mg g$^{-1}$ at 2.0 V in 27 mg L$^{-1}$ NaCl solution (Li et al., 2010). Later works found that building three-dimensional (3D) structure is an effective approach to alleviate the agglomeration of graphene sheets and shorten the diffusion distance (Xu et al., 2015a). For example, Shi et al. developed a hierarchical structure with the interconnected macropores within the graphene networks and nanopores on graphene sheets (Shi et al., 2016, 2019b). A high desalination capacity of 17.1 mg g$^{-1}$ was achieved at a cell potential of 1.6 V.

Metal-organic frameworks (MOFs), a new family of porous crystalline materials, have shown great promise as precursors of



**FIGURE 1 | (A)** Schematic diagram of capacitive deionization (CDI) structure. **(B)** Schematic diagram of Sodium-ion battery (SIB) structure.
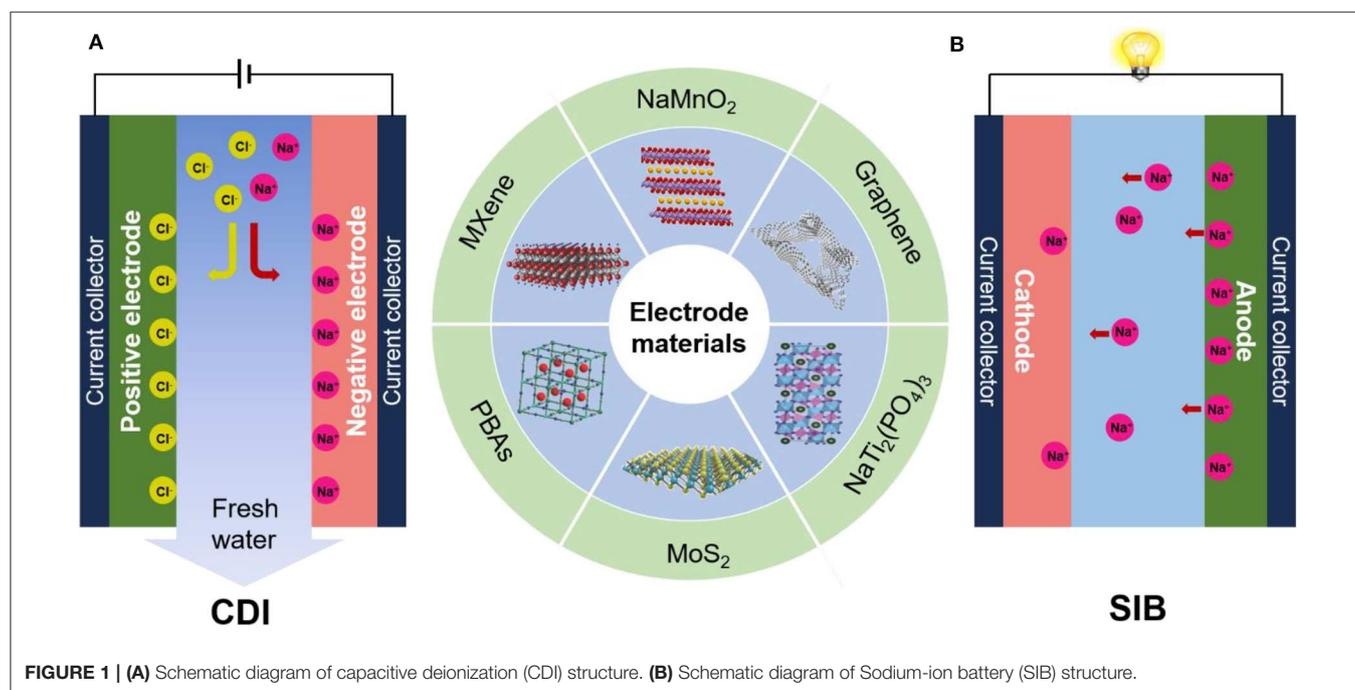
TABLE 1 | Performance comparison of the same material in CDI and SIB applications, respectively.

| Electrode materials | CDI performance | References | Energy storage performance | References |
|---|---|---|---|---|
| Graphene | 4.29 mg g$^{-1}$ at 2 V in 27 mg L$^{-1}$ NaCl | Li et al., 2010 | 50 mAh g$^{-1}$ at 6 A g$^{-1}$ in 1 M Na$_2$SO$_4$ 90% after 1,200 cycles at 6 A g$^{-1}$ | Li et al., 2012 |
| Meso-porous rGO nanosheet-assembled 3D graphene | 17.1 mg g$^{-1}$ at 1.6 V in 500 mg L$^{-1}$ NaCl | Shi et al., 2016 | 55.5 mAh g$^{-1}$ at 0.5 A g$^{-1}$ in 1 M Na$_2$SO$_4$ | Choi et al., 2012 |
| MOF-derived porous carbon | 13.86 mg g$^{-1}$ at 1.2 V in 500 mg L$^{-1}$ NaCl | Liu et al., 2015 | 109.7 mAh g$^{-1}$ at 0.2 A g$^{-1}$ in 500 mg L$^{-1}$ NaCl | Wang Z. et al., 2016 |
| Nitrogen-doped graphene sponge | 21.0 mg g$^{-1}$ at 1.2 V in 500 mg L$^{-1}$ NaCl ~100% after 30 cycles at 1.2 V | Xu et al., 2015b | 154 mAh g$^{-1}$ at 15 A g$^{-1}$ in 1 M NaClO$_4$ 99% after 7,000 cycles at 5 A g$^{-1}$ | Wang S. Q. et al., 2016 |
| Surface modified carbon | 16.7 mg g$^{-1}$ at 1 V in 30 mM NaCl | Gao et al., 2016 | 30.27 mAh g$^{-1}$ at 1.25 A g$^{-1}$ in 2 M Na$_2$SO$_4$ | Lang et al., 2012 |
| Na$_4$Mn$_9$O$_{18}$ | 31.2 mg g$^{-1}$ at 1.2 V in 50 mM NaCl | Lee et al., 2014 | 39 mAh g$^{-1}$ at 0.2 A g$^{-1}$ in 0.5 M Na$_2$SO$_4$ | Kim et al., 2013 |
| NaTi$_2$(PO$_4$)$_3$/rGO | 120 mg g$^{-1}$ at 100 mA g$^{-1}$ in 1,000 mg L$^{-1}$ NaCl 85.7% after 100 cycles at 100 mA g$^{-1}$ | Dong et al., 2017 | 58 mAh g$^{-1}$ at 0.5 A g$^{-1}$ in 1 M Na$_2$SO$_4$ 50% after 50 cycles at 0.5 A g$^{-1}$ | Zhang Q. et al., 2016 |
| Na$_3$V$_2$(PO$_4$)$_3$@C | 137.20 mg g$^{-1}$ at 1.0 V in 100 mM NaCl | Cao J. L. et al., 2019 | 58.1 mAh g$^{-1}$ at 1 A g$^{-1}$ in 1 M Na$_2$SO$_4$ 32% after 30 cycles at 1 A g$^{-1}$ | Song et al., 2014 |
| Wire Na$_3$V$_2$(PO$_4$)$_3$@C | 98 mg g$^{-1}$ at 100 mA g$^{-1}$ in 1,000 mg L$^{-1}$ NaCl 79% after 50 cycles at 100 mA g$^{-1}$ | Zhao et al., 2018 | 58.7 mAh g$^{-1}$ at 1 A g$^{-1}$ in 1 M Na$_2$SO$_4$ 83% after 600 cycles at A g$^{-1}$ | Dong et al., 2017 |
| Na$_3$V$_2$(PO$_4$)$_3$/graphene hybrid aerogel | 107.5 mg g$^{-1}$ at 100 mA g$^{-1}$ in 1,000 mg L$^{-1}$ NaCl 86.7% after 50 cycles at 100 mA g$^{-1}$ | Zhao W. Y. et al., 2019 | 92 mAh g$^{-1}$ at 50 mA g$^{-1}$ in 0.5 M CH$_3$COONa 77% after 200 cycles at 50 mA g$^{-1}$ | Li et al., 2016 |
| PBAs | 100 mg g$^{-1}$ at 2.8 A m$^{-2}$ in 50 mM NaCl 86% after 50 cycles at 5.7 A m$^{-2}$ | Kim et al., 2017 | 80 mAh g$^{-1}$ at 0.5 A g$^{-1}$ in 0.5 M Na$_2$SO$_4$ 93% after 8,000 cycles at 10 A g$^{-1}$ | Wang J. G. et al., 2017 |
| MXene | 45 mg g$^{-1}$ at 1.2 V in 10 g L$^{-1}$ NaCl Stable 60 cycles at 1.2 V | Bao et al., 2018 | 76.2 mAh g$^{-1}$ at 50 mA g$^{-1}$ in 1 M Na$_2$SO$_4$ 98% after 500 cycles at 0.2 A g$^{-1}$ | Zhu et al., 2017 |
| MoS$_2$ | 16.51 mg cm$^{-3}$ at 1.2 V in 400 mM NaCl | Xing et al., 2017 | 55 mAh g$^{-1}$ at 5 mV s$^{-1}$ in 1 M Na$_2$SO$_4$ 82% after 1,000 cycles | Pujari et al., 2017 |
| Na$_2$FeP$_2$O$_7$ | 30.2 mg g$^{-1}$ at 1.2 V in 100 mM NaCl | Kim et al., 2016 | 58 mAh g$^{-1}$ at 2 mA cm$^{-2}$ in 2 M Na$_2$SO$_4$ 89% after 30 cycles at 2 mA cm$^{-2}$ | Nakamoto et al., 2016 |
| V$_2$O$_5$ | 23.6 mg g$^{-1}$ at 100 mA g$^{-1}$ in 600 mM NaCl Stable 100 cycles at 100 mA g$^{-1}$ | Lee et al., 2017b | 119.1 mAh g$^{-1}$ at 1 A g$^{-1}$ in 1 M Na$_2$SO$_4$ 89.6% after 10,000 cycles at 20 mV s$^{-1}$ | Ghaly et al., 2019 |
| MnO$_2$ | 25.2 mg g$^{-1}$ at 5 A m$^{-2}$ in 0.1 M NaCl | Hand and Cusick, 2017 | 176 mAh g$^{-1}$ at 1 mA cm$^{-2}$ in 1 M Na$_2$SO$_4$ 95% after 2,000 cycles at 100 mV s$^{-1}$ | Chodankar et al., 2015 |

carbon-based materials. MOF-derived porous carbon materials have attracted much attentions in both energy storage devices and CDI, due to their large specific surface area and tunable microscopic structures (Xu et al., 2016; Shi et al., 2018). MOF-derived porous carbon was studied as the electrode of CDI for the first time by Pan et al. in 2015. Porous carbon obtained by direct carbonization of ZIF-8 exhibited a desalination capacity of 13.86 mg g$^{-1}$ at a cell potential of 1.2 V in 500 mg L$^{-1}$ NaCl solution. Since then, a large amount of MOF-derived carbon and their composites have been developed with further improved performance (Liu et al., 2015; Gao et al., 2019).

In addition, heteroatom doping can improve the wettability and conductivity of electrode materials, which is often adopted as a surface modification approach. Xu et al. synthesized a nitrogen-doped graphene sponge (NGS) as CDI electrode (Xu et al., 2015b). The NGS electrode with high specific surface area and superior electron mobility exhibited an ultrahigh desalination capacity of 21.0 mg g$^{-1}$ in 500 mg L$^{-1}$ NaCl solution. In order to get an insight into the mechanism of surface modification, Landon and co-workers synthesized functionalized carbon electrode and used it as a model to investigate the relationship between chemical surface charge and desalination performance (Gao et al., 2016). It was found that carbon electrodes with the optimized chemical surface charge can extend the working voltage window, thereby significantly increasing the desalination capacity of the CDI electrode.

Up to now, a large variety of investigations on structural design and surface modification of carbon-based materials have been conducted. There are many researchers engaged in the design, development, preparation, modification, and application of carbon materials. Undoubtedly, performance of CDI can be further enhanced via a further understanding of interfacial and kinetic properties of porous carbon materials in future.

# FARADAIC MATERIALS

Inspired by the energy storage systems, various faradaic electrode materials have been actively explored for water desalination in recent years. These materials allow the intercalation or redox reactions, which store ions in the bulk of electrode rather than capacitively stored on the surface. Therefore, they are promising for higher salt removal capability compared with conventional carbon materials (Cai et al., 2018).

Sodium manganese oxide, a layered structured material described as $Na_xMnO_2$ ($0 < x \leq 1$), has been intensively investigated in SIBs due to their high capacity and low cost. The pioneering work on the application of faradaic electrodes in water desalination was reported in 2012 (Pasta et al., 2012). Pasta et al. proposed a concept of desalination battery which is comprised by a $Na_{2-x}Mn_5O_{10}$ nanorod as positive electrode and Ag/AgCl as negative electrode. However, this system was mainly served as an energy storage device, salt removal only performed at static with a few hundreds of microliters of electrolyte. More recently, a hybrid CDI system was developed by combining a battery electrode ($Na_4Mn_9O_{18}$) with a capacitive electrode (activated carbon) demonstrating improved desalination capacity of 31.2 mg g$^{-1}$ as compared to traditional carbon-based CDI system (Lee et al., 2014).

Recently, sodium superionic conductors (NASICONs), such as $NaTi_2(PO_4)_3$ (NTP) (Huang et al., 2017, 2019; Guo et al., 2018; Wang et al., 2018; Zhang et al., 2020) and $Na_3V_2(PO_4)_3$ (NVP) (Cao J. L. et al., 2019; Cao X. X. et al., 2019), have been considered as promising cathode materials for sodium ion battery due to their high theoretical specific capacity and high Na$^+$ conductivity. Yang and co-workers fabricated a hybrid CDI cell with $NaTi_2(PO_4)_3$/rGO as positive electrode and activated carbon (AC) as negative electrode. During the desalination process, sodium ions are inserted into the NTP electrode, while chloride ions are adsorbed on the EDLs of AC electrode. An ultrahigh desalination capacity of 140 mg g$^{-1}$ in the first cycle was achieved at a current density of 100 mA g$^{-1}$, decreasing to 120 mg g$^{-1}$ after 100 cycle.

$Na_3V_2(PO_4)_3$ exhibits a high theoretical capacity (117.6 mAh g$^{-1}$) and good thermal stability. Cao et al. applied $Na_3V_2(PO_4)_3$@C as a novel faradaic electrode in a hybrid CDI system showing a desalination capacity of 137.30 mg g$^{-1}$ at a constant voltage of 1.0 V in 100 mM NaCl solution (Cao J. L. et al., 2019). Similar work was reported by Yang and co-workers, who synthesized a conductive polydopamine coated NVP (NVP@C) (Zhao et al., 2018). A faradaic CDI system was fabricated by coupling NVP@C as Na storage electrode and AgCl as Cl storage electrode via conversion reactions. Soon after, they reported a binder-free electrode for CDI, which is prepared from $Na_3V_2(PO_4)_3$/graphene hybrid aerogel (Zhao W. Y. et al., 2019).

Due to different sodium capture process of battery electrode as compared to carbon-based materials, battery electrode-based CDI can achieve higher desalination capacity and is also suitable to salty water with high concentration. Another distinct advantage of using battery electrode for CDI is that the co-ion effects of carbon electrode can be eliminated. Therefore, ion-exchange-membrane-free CDI can be achieved which are more compact and possible for miniature-size design. It is worth to mention that composite materials may be considered in future research. Based on the studies of SIBs, reasonable composite materials can improve the efficiency of ion and electron transport (Xu et al., 2017; Cai et al., 2018; Zhou et al., 2018). This strategy may be applied to enhance salt removal performance in CDI. Especially, some composite electrodes may be capable of combining the faradaic and EDLs adsorption principles to increase the amount of salt removal (Yue et al., 2019a). In addition, the concept of integrated and/or self-supported electrodes in SIBs can also be applied to the electrode design of CDI, which makes the preparation process simple and is possible for large-scale electrode production.

Prussian blue (PB) and its analogs (PBAs) with a general formula of $Na_xM_1[M_2(CN)_6]_y \cdot nH_2O$ (M: transition metal ions) are a family of coordination compounds with open framework structure. They have been widely investigated as alternative host materials in sodium ion capacitors, SIBs, and zinc-ion batteries in recent years (Qian et al., 2018). Benefiting from their unique large ionic channels and facile preparation, PB-based materials are promising electrode materials for CDI.

Lee et al. first designed a novel desalination system consisting two PBAs electrodes, i.e., the $Na_xNi[Fe(CN)_6]$ and $Na_xFe[Fe(CN)_6]$ electrodes with an anion exchange membrane in between. Based on the working principle of rocking chair battery, this system achieved efficient desalination during charging and discharging, with a desalination capacity of 59.9 mg g$^{-1}$ (Lee et al., 2017a).

Soon after, Guo et al. assembled a hybrid CDI cell using $FeFe(CN)_6$ crystals as positive electrode and AC as negative electrode. The PB crystals prepared by a simple chemical precipitation method undergo reversible Na$^+$ insertion/extraction process as the following redox reaction.

$$xNa^+ + xe^- + FeFe(CN)_6 \leftrightarrow Na_xFeFe(CN)_6$$

The hybrid CDI cell delivered a high removal capacity of 101.7 mg g$^{-1}$ at a current density of 0.125 mA g$^{-1}$ and good cycling stability (Guo et al., 2017).

Later, Choi et al. conducted a similar study to synthesize a CuFe-PBA framework ($K_{0.03}Cu[Fe(CN)_6]_{0.65} \cdot 0.43H_2O$) which is coupled with porous carbon in a hybrid CDI cell. Besides Na$^+$ ions, effective removal of various cations such as K$^+$, Mg$^{2+}$, and Ca$^{2+}$ was also demonstrated, showing potential application toward desalination of complex feed waters (Choi et al., 2018).

Along with the exploration of new PB crystals, various strategies of structural and morphological modifications have also been developed to further improve their CDI performance. For example, to enhance the electronic conductivity of the PBs, Vafakhah et al. reported a PB/rGO aerogel by embedding PB nanocubes in rGO 3D networks and applied them in a hybrid CDI system. Compared with pristine PB particles, the PB/rGO composite exhibited a noticeably higher desalination capacity of 130 mg g$^{-1}$ at the current density of 100 mA g$^{-1}$ and higher rate capability. At the same time, the reversible intercalation/de-intercalation mechanism of PB-based electrode was further confirmed by *in-situ* XRD analysis (Vafakhah

et al., 2019). In addition, Zhao et al. designed a core–shell structured CuFe-PBA@NiFe-PBA, which combines the high capacity of CuFe-PBA core with highly stable NiFe-PBA shell. This core-shelled PBA material delivered $71.8 \pm 2.0$ mg g$^{-1}$ at 0.5 mA cm$^{-2}$, which is over 32% higher than those of CuFe-PBA and NiFe-PBA, respectively (Zhao Y. B. et al., 2019).

Although their potential advantages, PB-based materials suffer from unsatisfactory performance which is mainly caused by a large amount of lattice defects and coordinated water. The defects largely reduce the utilization of redox-active sites in the PB framework that allow sodium storage, thus leading to a low salt removal capacity. Therefore, in the future research of PB-based CDI electrodes, efforts can be made to develop high-crystallinity PB electrode materials. In addition, related researches on SIBs have revealed that particle size of PBA crystals has significant influence on ion diffusion rate and the rate performance. This finding is also important for the desalination rate of CDI. Unfortunately, nano-sized PB normally has higher surface defect density, a possible solution is to rationally construct composite electrode with the integrity of crystal structure of PBA maintaining.

The breakthrough of graphene has promoted intensive researches on two-dimensional (2D) nanomaterials in past decades. The emerging new types of 2D nanomaterials and their composites have been widely used in various fields including electrochemical energy storage (Liu et al., 2019b, 2020; Zhao H. W. et al., 2019; Wu et al., 2020). MXene, first reported by Naguib et al., is a family of layer structured metal carbide/nitride which shares a general formula of $M_{n+1}AX_n$ (M is early transition metal, A is an element of group IIIA and IVA, X is C and/or N). After selective etching of A layers, the exfoliated MXene layer with ultrathin thickness is a promising 2D material (Naguib et al., 2011). Compared with other 2D materials such as graphene, MXene has unique advantages of abundant functional groups and tunable properties owing to various chemical composition and controllable interlayer space (VahidMohammadi et al., 2019). MXenes have been proved promising for efficient sodium storage, especially in SIBs and capacitors, delivering specific capacities of 30–76.2 mAh g$^{-1}$ (Zhu et al., 2017; Guan et al., 2020).

Srimuk et al. first reported the application of MXene in a symmetrical CDI cell prepared by direct casting of Ti$_3$C$_2$ onto a porous separator without addition of binder. The fabricated CDI cell demonstrated a desalinization capacity of more than 13 mg g$^{-1}$ in 5 mM NaCl solution, which is comparable to most of conventional carbon materials for CDI (Srimuk et al., 2016). The relatively low capacity maybe due to the restacking of MXene sheets.

Later, Bao et al. prepared an aerogel-like porous Ti$_3$C$_2$T$_x$ MXene electrode by vacuum freeze-drying process. Impressively, the porous MXene demonstrated a high volumetric salt removal capacity of 118 mg cm$^{-3}$ which is attributed to effective utilization of the 2D surfaces (Bao et al., 2018). Similarly, Ma et al. prepared a free-standing Ti$_3$C$_2$T$_x$ MXene film as binder-free electrode for CDI (Sriramulu and Yang, 2019). Recently, it was found that the introduction of heteroatom dopants to MXene

can effectively improve the electronic conductivity and reduce the risk of restacking as well (Amiri et al., 2020).

As a CDI electrode, MXene has the following competitive advantages. First, MXene has intrinsically high volumetric capacitance, enabling high desalination capacity. Second, MXene is accessible to other types of ions beyond Na, which makes it possible for applications in real feedwater (Lukatskaya et al., 2013; Come et al., 2015). In addition, as a typical 2D layered material, MXene has the common feature of strong attraction between layers. Therefore, it can be used as a binder-free electrode, which has appealing advantage for miniature and portable CDI devices. However, most of etching processes of MXene involve the toxic HF which limits the large-scale preparation of MXene in CDI. In future, the etching method need to be further developed to fulfill the requirements of commercial applications.

Another attractive 2D material is few-layered MoS$_2$ sheets or flakes, which have been insensitively studied as anode material for SIBs (Sun et al., 2018). Recently, CDI performance of chemically exfoliated MoS$_2$ (ce-MoS$_2$) nanosheets were investigated by Cao and co-workers (Xing et al., 2017). The ce-MoS$_2$ nanosheets demonstrated a good cycling stability and a desalination capacity of 8.81 mg g$^{-1}$ at 1.2 V in 400 mM NaCl solution. MoS$_2$ as CDI electrode cannot give a satisfactory performance, possibly due to the poor conductivity and low accessible active sites. Shortly afterward, various low dimensional nanomaterials such as CNT (Srimuk et al., 2017), graphene (Han J. L. et al., 2019; Peng et al., 2020), or g-C$_3$N$_4$ (Tian et al., 2020) were employed to further improve the performance of MoS$_2$.

MoS$_2$ can be obtained from a naturally abundant mineral by a simple exfoliation method, which is a low-cost electrode for CDI. However, it is difficult to control the number of layers of the obtained MoS$_2$ sheets, which greatly affects the ion diffusion process and leads to rapid capacity fading. Further work is recommended to investigate the relationship between thickness and desalination performance of MoS$_2$.

In addition, other commonly used battery electrode materials have also been applied in CDI, such as Na$_2$FeP$_2$O$_7$ (Kim et al., 2016), multi walled CNT/hV$_2$O$_5$ composite (Lee et al., 2017b), and MnO$_2$ (Hand and Cusick, 2017).

## SUMMARY

In summary, CDI is an emerging water treatment technology which shares many similarities with electrochemical energy storage systems. In the near future, the CDI research community is expected to grow larger with the development of novel electrode materials and cell architectures. Obviously, CDI has many advantages over other desalination technologies, including mild operation conditions with no high pressure and heat source required, simple cell configuration, low-cost and high energy efficiency for low salinity streams. However, it is still facing great challenges of application in real feedwaters. More efforts can be made in future to the investigation of electrode materials capable of capturing multivalent ions. Moreover, the adsorption behavior of soluble organics in water is more complicated, which may

cause biofouling and affect the desalination performance and service life of CDI.

Another future direction of CDI technology may be the combination with renewable energy resources, such as solar energy and wind energy, to reduce the energy consumption. For example, a recent work demonstrated a flow-electrode CDI system with low energy consumption (Desai et al., 2018). It is also promising to develop miniaturized and portable desalination devices which may have potential applications in exploration and disaster-affected area.

The adsorption of chloride ions will also affect the desalination performance of the whole device. Although silver has been investigated for $Cl^-$ ion storage (Yue et al., 2019b), high cost of silver limits its large-scale application in water treatment. Other types of materials, such as bismuth, may be considered. Moreover, researchers may also pay attention to relevant achievements in the recent developed chloride ion battery (Pasta et al., 2012; Nam and Choi, 2017).

In addition, the salt removal mechanism of many recently developed battery electrode materials is different from the generally accepted EDLs principle. Therefore, combining *in-situ* technology to reveal the correlation between the structure of battery electrode materials and its corresponding desalination performance, as well as the desalination mechanism of novel battery materials is another interesting research direction.

## AUTHOR CONTRIBUTIONS

WS, XG, JM, XQ, WL, FW, HL, ZZ, JS, and XC contributed to the discussion and writing in this work.

## FUNDING

## REFERENCES

Amiri, A., Chen, Y. J., Teng, C. B., and Naraghi, M. (2020). Porous nitrogen-doped MXene-based electrodes for capacitive deionization. *Energy Storage Mater.* 25, 731–739. doi: 10.1016/j.ensm.2019.09.013

Balogun, M. S., Luo, Y., Qiu, W. T., Liu, P., and Tong, Y. X. (2016). A review of carbon materials and their composites with alloy metals for sodium ion battery anodes. *Carbon N.Y.* 98, 162–178. doi: 10.1016/j.carbon.2015.09.091

Bao, W. Z., Tang, X., Guo, X., Choi, S., Wang, C. Y., Gogotsi, Y., et al. (2018). Porous cryo-dried mxene for efficient capacitive deionization. *Joule* 2, 778–787. doi: 10.1016/j.joule.2018.02.018

Bharath, G., Alhseinat, E., Ponpandian, N., Khan, M. A., Siddiqui, M. R., Ahmed, F., et al. (2017). Development of adsorption and electrosorption techniques for removal of organic and inorganic pollutants from wastewater using novel magnetite/porous graphene-based nanocomposites. *Sep. Purif. Technol.* 188, 206–218. doi: 10.1016/j.seppur.2017.07.024

Cai, Y. S., Cao, X. X., Luo, Z. G., Fang, G. Z., Liu, F., Zhou, J., et al. (2018). Caging $Na_3V_2(PO_4)_2F_3$ microcubes in cross-linked graphene enabling ultrafast sodium storage and long-term cycling. *Adv. Sci.* 5:10. doi: 10.1002/advs.201800680

Cao, J. L., Wang, Y., Wang, L., Yu, F., and Ma, J. (2019). $Na_3V_2(PO_4)_3$@C as faradaic electrodes in capacitive deionization for high-performance desalination. *Nano Lett.* 19, 823–828. doi: 10.1021/acs.nanolett.8b04006

Cao, X. X., Pan, A. Q., Yin, B., Fang, G. Z., Wang, Y. P., Kong, X. Z., et al. (2019). Nanoflake-constructed porous $Na_3V_2(PO_4)_3$/C hierarchical microspheres as a bicontinuous cathode for sodium-ion batteries applications. *Nano Energy* 60, 312–323. doi: 10.1016/j.nanoen.2019.03.066

Chao, D. L., Ouyang, B., Liang, P., Huong, T. T. T., Jia, G. C., Huang, H., et al. (2018). C-Plasma of hierarchical graphene survives SnS bundles for ultrastable and high volumetric Na-Ion storage. *Adv. Mater.* 30:6. doi: 10.1002/adma.201804833

Chodankar, N. R., Dubal, D. P., Gund, G. S., and Lokhande, C. D. (2015). Flexible all-solid-state $MnO_2$ thin films based symmetric supercapacitors. *Electrochim. Acta* 165, 338–347. doi: 10.1016/j.electacta.2015.02.246

Choi, B. G., Yang, M., Hong, W. H., Choi, J. W., and Huh, Y. S. (2012). 3D macroporous graphene frameworks for supercapacitors with high energy and power densities. *ACS Nano* 6, 4020–4028. doi: 10.1021/nn3003345

Choi, S., Chang, B., Kim, S., Lee, J., Yoon, J., and Choi, J. W. (2018). Battery electrode materials with omnivalent cation storage for fast and charge-efficient ion removal of asymmetric capacitive deionization. *Adv. Funct. Mater.* 28:9. doi: 10.1002/adfm.201802665

Come, J., Black, J. M., Lukatskaya, M. R., Naguib, M., Beidaghi, M., Rondinone, A. J., et al. (2015). Controlling the actuation properties of MXene paper electrodes upon cation intercalation. *Nano Energy* 17, 27–35. doi: 10.1016/j.nanoen.2015.07.028

Delmas, C. (2018). Sodium and sodium-ion batteries: 50 years of research. *Adv. Energy Mater.* 8:9. doi: 10.1002/aenm.201703137

Desai, D., Beh, E. S., Sahu, S., Vedharathinam, V., van Overmeere, Q., de Lannoy, C. F., et al. (2018). Electrochemical desalination of seawater and hypersaline brines with coupled electricity storage. *Acs Energy Lett.* 3, 375–379. doi: 10.1021/acsenergylett.7b01220

Dong, J., Zhang, G. M., Wang, X. G., Zhang, S., and Deng, C. (2017). Cross-linked $Na_2VTi(PO_4)_3$@C hierarchical nanofibers as high-performance bi-functional electrodes for symmetric aqueous rechargeable sodium batteries. *J. Mater. Chem. A* 5, 18725–18736. doi: 10.1039/C7TA05361D

Fang, G. Z., Wang, Q. C., Zhou, J., Lei, Y. P., Chen, Z. X., Wang, Z. Q., et al. (2019). Metal organic framework-templated synthesis of bimetallic selenides with rich phase boundaries for sodium-ion storage and oxygen evolution reaction. *ACS Nano* 13, 5635–5645. doi: 10.1021/acsnano.9b00816

Fang, G. Z., Wu, Z. X., Zhou, J., Zhu, C. Y., Cao, X. X., Lin, T. Q., et al. (2018). Observation of pseudocapacitive effect and fast ion diffusion in bimetallic sulfides as an advanced sodium-ion battery anode. *Adv. Energy Mater.* 8:10. doi: 10.1002/aenm.201703155

Farmer, J. C., Fix, D. V., Mack, G. V., Pekala, R. W., and Poco, J. F. (1996). Capacitive deionization of NaCl and $NaNO_3$ solutions with carbon aerogel electrodes. *J. Electrochem. Soc.* 143, 159–169. doi: 10.1149/1.1836402

Gao, T., Li, H. B., Zhou, F., Gao, M. M., Liang, S., and Luo, M. (2019). Mesoporous carbon derived from ZIF-8 for high efficient electrosorption. *Desalination* 451, 133–138. doi: 10.1016/j.desal.2017.06.021

Gao, X., Omosebi, A., Landon, J., and Liu, K. L. (2015). Surface charge enhanced carbon electrodes for stable and efficient capacitive deionization using inverted adsorption-desorption behavior. *Energy Environ. Sci.* 8, 897–909. doi: 10.1039/C4EE03172E

Gao, X., Porada, S., Omosebi, A., Liu, K. L., Biesheuvel, P. M., and Landon, J. (2016). Complementary surface charge for enhanced capacitive deionization. *Water Res.* 92, 275–282. doi: 10.1016/j.watres.2016.01.048

Ghaly, H. A., El-Deen, A. G., Souaya, E. R., and Allam, N. K. (2019). Asymmetric supercapacitors based on 3D graphene-wrapped $V_2O_5$ nanospheres and

Fe$_3$O$_4$@3D graphene electrodes with high power and energy densities. *Electrochim. Acta* 310, 58–69. doi: 10.1016/j.electacta.2019.04.071

Guan, Y. F., Jiang, S., Cong, Y., Wang, J. P., Dong, Z. J., Zhang, Q., et al. (2020). A hydrofluoric acid-free synthesis of 2D vanadium carbide (V2C) MXene for supercapacitor electrodes. *2D Mater.* 7:9. doi: 10.1088/2053-1583/ab6706

Guo, L., Mo, R. W., Shi, W. H., Huang, Y. X., Leong, Z. Y., Ding, M., et al. (2017). A prussian blue anode for high performance electrochemical deionization promoted by the faradaic mechanism. *Nanoscale* 9, 13305–13312. doi: 10.1039/C7NR03579A

Guo, Z. W., Ma, Y. Y., Dong, X. L., Hou, M. Y., Wang, Y. G., and Xia, Y. Y. (2018). Integrating desalination and energy storage using a saltwater-based hybrid sodium-ion supercapacitor. *ChemSusChem* 11, 1741–1745. doi: 10.1002/cssc.201800517

Han, J. L., Yan, T. T., Shen, J. J., Shi, L. Y., Zhang, J. P., and Zhang, D. S. (2019). Capacitive Deionization of saline water by using MoS$_2$-graphene hybrid electrodes with high volumetric adsorption capacity. *Environ. Sci. Technol.* 53, 12668–12676. doi: 10.1021/acs.est.9b04274

Han, Y., Lu, Y. Z., Shen, S. H., Zhong, Y., Liu, S., Xia, X. H., et al. (2019). Enhancing the capacitive storage performance of carbon fiber textile by surface and structural modulation for advanced flexible asymmetric supercapacitors. *Adv. Funct. Mater.* 29:9. doi: 10.1002/adfm.201806329

Hand, S., and Cusick, R. D. (2017). Characterizing the impacts of deposition techniques on the performance of MnO$_2$ cathodes for sodium electrosorption in hybrid capacitive deionization. *Environ. Sci. Technol.* 51, 12027–12034. doi: 10.1021/acs.est.7b03060

Huang, Y. X., Chen, F. M., Guo, L., and Yang, H. Y. (2017). Ultrahigh performance of a novel electrochemical deionization system based on a NaTi$_2$(PO$_4$)$_3$/rGO nanocomposite. *J. Mater. Chem. A* 5, 18157–18165. doi: 10.1039/C7TA03725B

Huang, Y. X., Chen, F. M., Guo, L., Zhang, J., Chen, T. P., and Yang, H. Y. (2019). Low energy consumption dual-ion electrochemical deionization system using NaTi$_2$(PO$_4$)$_3$-AgNPs electrodes. *Desalination* 451, 241–247. doi: 10.1016/j.desal.2018.02.006

Huang, Z., Lu, L., Cai, Z. X., and Ren, Z. J. (2016). Individual and competitive removal of heavy metals using capacitive deionization. *J. Hazard. Mater.* 302, 323–331. doi: 10.1016/j.jhazmat.2015.09.064

Kim, D. J., Ponraj, R., Kannan, A. G., Lee, H. W., Fathi, R., Ruffo, R., et al. (2013). Diffusion behavior of sodium ions in Na$_{0.44}$MnO$_2$ in aqueous and non-aqueous electrolytes. *J. Power Sources* 244, 758–763. doi: 10.1016/j.jpowsour.2013.02.090

Kim, H., Hong, J., Park, K. Y., Kim, H., Kim, S. W., and Kang, K. (2014). Aqueous rechargeable Li and Na ion batteries. *Chem. Rev.* 114, 11788–11827. doi: 10.1021/cr500232y

Kim, S., Lee, J., Kim, C., and Yoon, J. (2016). Na$_2$FeP$_2$O$_7$ as a novel material for hybrid capacitive deionization. *Electrochim. Acta* 203, 265–271. doi: 10.1016/j.electacta.2016.04.056

Kim, T., Gorski, C. A., and Logan, B. E. (2017). Low energy desalination using battery electrode deionization. *Environ. Sci. Technol. Lett.* 4, 444–449. doi: 10.1021/acs.estlett.7b00392

Lang, J. W., Yan, X. B., Liu, W. W., Wang, R. T., and Xue, Q. J. (2012). Influence of nitric acid modification of ordered mesoporous carbon materials on their capacitive performances in different aqueous electrolytes. *J. Power Sources* 204, 220–229. doi: 10.1016/j.jpowsour.2011.12.044

Lee, J., Kim, S., Kim, C., and Yoon, J. (2014). Hybrid capacitive deionization to enhance the desalination performance of capacitive techniques. *Energy Environ. Sci.* 7, 3683–3689. doi: 10.1039/C4EE02378A

Lee, J., Kim, S., and Yoon, J. (2017a). Rocking chair desalination battery based on prussian blue electrodes. *ACS Omega* 2, 1653–1659. doi: 10.1021/acsomega.6b00526

Lee, J., Srimuk, P., Aristizabal, K., Kim, C., Choudhury, S., Nah, Y. C., et al. (2017b). Pseudocapacitive desalination of brackish water and seawater with vanadium-pentoxide-decorated multiwalled carbon nanotubes. *ChemSusChem* 10, 3611–3623. doi: 10.1002/cssc.201701215

Li, G. L., Yang, Z., Jiang, Y., Zhang, W. X., and Huang, Y. H. (2016). Hybrid aqueous battery based on Na$_3$V$_2$(PO$_4$)$_3$/C cathode and zinc anode for potential large-scale energy storage. *J. Power Sources* 308, 52–57. doi: 10.1016/j.jpowsour.2016.01.058

Li, H. B., Zou, L. D., Pan, L. K., and Sun, Z. (2010). Novel graphene-like electrodes for capacitive deionization. *Environ. Sci. Technol.* 44, 8692–8697. doi: 10.1021/es101888j

Li, J., Wang, X. X., Wang, H. Q., Wang, S. H., Hayat, T., Alsaedi, A., et al. (2017). Functionalization of biomass carbonaceous aerogels and their application as electrode materials for electro-enhanced recovery of metal ions. *Environ. Sci. Nano* 4, 1114–1123. doi: 10.1039/C7EN00019G

Li, Z. J., Yang, B. C., Zhang, S. R., and Zhao, C. M. (2012). Graphene oxide with improved electrical conductivity for supercapacitor electrodes. *Appl. Surf. Sci.* 258, 3726–3731. doi: 10.1016/j.apsusc.2011.12.015

Liu, W., Yu, L., Yin, R., Xu, X., Feng, J., Jiang, X., et al. (2020). Non-3d metal modulation of a 2D Ni-Co heterostructure array as multifunctional electrocatalyst for portable overall water splitting. *Small* 16:e1906775. doi: 10.1002/smll.201906775

Liu, W. X., Yin, R. L., Shi, W. H., Xu, X. L., Shen, X. H., Yin, Q. C., et al. (2019a). Gram-scale preparation of 2D transition metal hydroxide/oxide assembled structures for oxygen evolution and Zn-Air battery. *ACS Appl. Energy Mater.* 2, 579–586. doi: 10.1021/acsaem.8b01613

Liu, W. X., Yin, R. L., Xu, X. L., Zhang, L., Shi, W. H., and Cao, X. H. (2019b). Structural engineering of low-dimensional metal-organic frameworks: synthesis, properties, and applications. *Adv. Sci.* 6:32. doi: 10.1002/advs.201802373

Liu, Y., Xu, X. T., Wang, M., Lu, T., Sun, Z., and Pan, L. K. (2015). Metal-organic framework-derived porous carbon polyhedra for highly efficient capacitive deionization. *Chem. Commun.* 51, 12020–12023. doi: 10.1039/C5CC03999A

Lukatskaya, M. R., Mashtalir, O., Ren, C. E., Dall'Agnese, Y., Rozier, P., Taberna, P. L., et al. (2013). Cation intercalation and high volumetric capacitance of two-dimensional titanium carbide. *Science* 341, 1502–1505. doi: 10.1126/science.1241488

Naguib, M., Kurtoglu, M., Presser, V., Lu, J., Niu, J. J., Heon, M., et al. (2011). Two-dimensional nanocrystals produced by exfoliation of Ti$_3$AlC$_2$. *Adv. Mater.* 23, 4248–4253. doi: 10.1002/adma.201102306

Nakamoto, K., Kano, Y., Kitajou, A., and Okada, S. (2016). Electrolyte dependence of the performance of a Na$_2$FeP$_2$O$_7$//NaTi$_2$(PO$_4$)$_3$ rechargeable aqueous sodium-ion battery. *J. Power Sources* 327, 327–332. doi: 10.1016/j.jpowsour.2016.07.052

Nam, D. H., and Choi, K. S. (2017). Bismuth as a new chloride-storage electrode enabling the construction of a practical high capacity desalination battery. *J. Am. Chem. Soc.* 139, 11055–11063. doi: 10.1021/jacs.7b01119

Noonan, O., Liu, Y., Huang, X., and Yu, C. (2018). Layered graphene/mesoporous carbon heterostructures with improved mesopore accessibility for high performance capacitive deionization. *J. Mater. Chem. A* 6, 14272–14280. doi: 10.1039/C8TA03114B

Oladunni, J., Zain, J. H., Hai, A., Banat, F., Bharath, G., and Alhseinat, E. (2018). A comprehensive review on recently developed carbon based nanocomposites for capacitive deionization: from theory to practice. *Sep. Purif. Technol.* 207, 291–320. doi: 10.1016/j.seppur.2018.06.046

Panwar, N. L., Kaushik, S. C., and Kothari, S. (2011). Role of renewable energy sources in environmental protection: a review. *Ren. Sust. Energy Rev.* 15, 1513–1524. doi: 10.1016/j.rser.2010.11.037

Pasta, M., Wessells, C. D., Cui, Y., and La Mantia, F. (2012). A desalination battery. *Nano Lett.* 12, 839–843. doi: 10.1021/nl203889e

Peng, W. J., Wang, W., Han, G. H., Huang, Y. K., and Zhang, Y. S. (2020). Fabrication of 3D flower-like MoS2/graphene composite as high-performance electrode for capacitive deionization. *Desalination* 473:11. doi: 10.1016/j.desal.2019.114191

Porada, S., Borchardt, L., Oschatz, M., Bryjak, M., Atchison, J. S., Keesman, K. J., et al. (2013). Direct prediction of the desalination performance of porous carbon electrodes for capacitive deionization. *Energy Environ. Sci.* 6, 3700–3712. doi: 10.1039/c3ee42209g

Pujari, R. B., Lokhande, A. C., Shelke, A. R., Kim, J. H., and Lokhande, C. D. (2017). Chemically deposited nano grain composed MoS$_2$ thin films for supercapacitor application. *J. Colloid Interface Sci.* 496, 1–7. doi: 10.1016/j.jcis.2016.11.026

Qian, J., Wu, C., Cao, Y., Ma, Z., Huang, Y., Ai, X., et al. (2018). Prussian blue cathode materials for sodium-ion batteries and other ion batteries. *Adv. Energy Mater.* 8:1702619. doi: 10.1002/aenm.201702619

Raza, W., Ali, F. Z., Raza, N., Luo, Y. W., Kim, K. H., Yang, J. H., et al. (2018). Recent advancements in supercapacitor technology. *Nano Energy* 52, 441–473. doi: 10.1016/j.nanoen.2018.08.013

Shahzad, M. W., Burhan, M., Ang, L., and Ng, K. C. (2017). Energy-water-environment nexus underpinning future desalination sustainability. *Desalination* 413, 52–64. doi: 10.1016/j.desal.2017.03.009

Shi, W. H., Li, H. B., Cao, X. H., Leong, Z. Y., Zhang, J., Chen, T. P., et al. (2016). Ultrahigh performance of novel capacitive deionization electrodes based on a three-dimensional graphene architecture with nanopores. *Sci. Rep.* 6:9. doi: 10.1038/srep18966

Shi, W. H., Liu, X. Y., Ye, C. Z., Cao, X. H., Gao, C. J., and Shen, J. N. (2019a). Efficient lithium extraction by membrane capacitive deionization incorporated with monovalent selective cation exchange membrane. *Sep. Purif. Technol.* 210, 885–890. doi: 10.1016/j.seppur.2018.09.006

Shi, W. H., Mao, J., Xu, X. L., Liu, W. X., Zhang, L., Cao, X. H., et al. (2019b). An ultra-dense NiS2/reduced graphene oxide composite cathode for high-volumetric/gravimetric energy density nickel-zinc batteries. *J. Mater. Chem. A* 7, 15654–15661. doi: 10.1039/C9TA04900B

Shi, W. H., Xu, X. L., Ye, C. Z., Sha, D. Y., Yin, R. L., Shen, X. H., et al. (2019c). Bimetallic metal-organic framework-derived carbon nanotube-based frameworks for enhanced capacitive deionization and Zn-Air battery. *Front. Chem.* 7:10. doi: 10.3389/fchem.2019.00449

Shi, W. H., Ye, C. Z., Xu, X. L., Liu, X. Y., Ding, M., Liu, W. X., et al. (2018). High-performance membrane capacitive deionization based on metal-organic framework-derived hierarchical carbon structures. *ACS Omega* 3, 8506–8513. doi: 10.1021/acsomega.8b01356

Song, W. X., Ji, X. B., Zhu, Y. R., Zhu, H. J., Li, F. Q., Chen, J., et al. (2014). Aqueous sodium-ion battery using a Na3V2(PO4)3 electrode. *ChemElectroChem* 1, 871–876. doi: 10.1002/celc.201300248

Srimuk, P., Kaasik, F., Kruner, B., Tolosa, A., Fleischmann, S., Jackel, N., et al. (2016). MXene as a novel intercalation-type pseudocapacitive cathode and anode for capacitive deionization. *J. Mater. Chem. A* 4, 18265–18271. doi: 10.1039/C6TA07833H

Srimuk, P., Lee, J., Fleischmann, S., Choudhury, S., Jackel, N., Zeiger, M., et al. (2017). Faradaic deionization of brackish and sea water via pseudocapacitive cation and anion intercalation into few-layered molybdenum disulfide. *J. Mater. Chem. A* 5, 15640–15649. doi: 10.1039/C7TA03120C

Sriramulu, D., and Yang, H. Y. (2019). Free-standing flexible film as a binder-free electrode for an efficient hybrid deionization system. *Nanoscale* 11, 5896–5908. doi: 10.1039/C8NR09119F

Sun, D., Ye, D. L., Liu, P., Tang, Y. G., Guo, J., Wang, L. Z., et al. (2018). MoS2/Graphene nanosheets from commercial bulky MoS2 andgraphite as anode materials for high rate sodium-ion batteries. *Adv. Energy Mater.* 8:11. doi: 10.1002/aenm.201702383

Suss, M., Porada, S., Sun, X., Biesheuvel, P., Yoon, J., and Presser, V. (2015). Water desalination via capacitive deionization: what is it and what can we expect from it? *Energy Environ. Sci.* 8, 2296–2319. doi: 10.1039/C5EE00519A

Tang, W. W., Liang, J., He, D., Gong, J. L., Tang, L., Liu, Z. F., et al. (2019). Various cell architectures of capacitive deionization: recent advances and future trends. *Water Res.* 150, 225–251. doi: 10.1016/j.watres.2018.11.064

Tian, S., Zhang, X., and Zhang, Z. (2020). Capacitive deionization with MoS2/g-C3N4 electrodes. *Desalination* 479:114348. doi: 10.1016/j.desal.2020.114348

Vafakhah, S., Guo, L., Sriramulu, D., Huang, S. Z., Saeedikhani, M., and Yang, H. Y. (2019). Efficient sodium-ion intercalation into the freestanding prussian blue/graphene aerogel anode in a hybrid capacitive deionization system. *ACS Appl. Mater. Interfaces* 11, 5989–5998. doi: 10.1021/acsami.8b18746

VahidMohammadi, A., Mojtabavi, A., Caffrey, N. M., Wanunu, M., and Beidaghi, M. (2019). Assembling 2D mxenes into highly stable pseudocapacitive electrodes with high power and energy densities. *Adv. Mater.* 31:9. doi: 10.1002/adma.201806931

Wang, J. G., Zhang, Z. Y., Zhang, X. Y., Yin, X. M., Li, X., Liu, X. R., et al. (2017). Cation exchange formation of prussian blue analogue submicroboxes for high-performance Na-ion hybrid supercapacitors. *Nano Energy* 39, 647–653. doi: 10.1016/j.nanoen.2017.07.055

Wang, L., and Lin, S. H. (2019). Mechanism of selective ion removal in membrane capacitive deionization for water softening. *Environ. Sci. Technol.* 53, 5797–5804. doi: 10.1021/acs.est.9b00655

Wang, L. B., Mu, C. N., Li, H. X., and Li, F. J. (2018). A dual-function battery for desalination and energy storage. *Inorg. Chem. Front.* 5, 2522–2526. doi: 10.1039/C8QI00704G

Wang, S. Q., Xia, L., Yu, L., Zhang, L., Wang, H. H., and Lou, X. W. (2016). Free-standing nitrogen-doped carbon nanofiber films: integrated electrodes for sodium-ion batteries with ultralong cycle life and superior rate capability. *Adv. Energy Mater.* 6:7. doi: 10.1002/aenm.201670044

Wang, Z., Yan, T. T., Fang, J. H., Shi, L. Y., and Zhang, D. S. (2016). Nitrogen-doped porous carbon derived from a bimetallic metal-organic framework as highly efficient electrodes for flow-through deionization capacitors. *J. Mater. Chem. A* 4, 10858–10868. doi: 10.1039/C6TA02420C

Wang, Z. J., Gong, H., Zhang, Y., Liang, P., and Wang, K. J. (2017). Nitrogen recovery from low-strength wastewater by combined membrane capacitive deionization (MCDI) and ion exchange (IE) process. *Chem. Eng. J.* 316, 1–6. doi: 10.1016/j.cej.2017.01.082

Wu, F., Gao, X., Xu, X., Jiang, Y., Gao, X., Yin, R., et al. (2020). MnO2 nanosheet-assembled hollow polyhedron grown on carbon cloth for flexible aqueous zinc-ion batteries. *ChemSusChem* 13, 1537–1545. doi: 10.1002/cssc.201903006

Xing, F., Li, T., Li, J. Y., Zhu, H. R., Wang, N., and Cao, X. (2017). Chemically exfoliated MoS2 for capacitive deionization of saline water. *Nano Energy* 31, 590–595. doi: 10.1016/j.nanoen.2016.12.012

Xu, X. L., Shi, W. H., Li, P., Ye, S. F., Ye, C. Z., Ye, H. J., et al. (2017). Facile fabrication of three-dimensional graphene and metal-organic framework composites and their derivatives for flexible all-solid-state supercapacitors. *Chem. Mater.* 29, 6058–6065. doi: 10.1021/acs.chemmater.7b01947

Xu, X. L., Shi, W. H., Liu, W. X., Ye, S. F., Yin, R. L., Zhang, L., et al. (2018). Preparation of two-dimensional assembled NiMn-C ternary composites for high-performance all-solid-state flexible supercapacitors. *J. Mater. Chem. A* 6, 24086–24091. doi: 10.1039/C8TA06412A

Xu, X. T., Li, J. L., Wang, M., Liu, Y., Lu, T., and Pan, L. K. (2016). Shuttle-like porous carbon rods from carbonized metal-organic frameworks for high-performance capacitive deionization. *ChemElectroChem* 3, 993–998. doi: 10.1002/celc.201600051

Xu, X. T., Pan, L. K., Liu, Y., Lu, T., Sun, Z., and Chua, D. H. C. (2015a). Facile synthesis of novel graphene sponge for high performance capacitive deionization. *Sci. Rep.* 5:9. doi: 10.1038/srep08458

Xu, X. T., Sun, Z., Chua, D. H. C., and Pan, L. K. (2015b). Novel nitrogen doped graphene sponge with ultrahigh capacitive deionization performance. *Sci. Rep.* 5:9. doi: 10.1038/srep11225

Yue, Z. S., Gao, T., and Li, H. B. (2019a). Robust synthesis of carbon@Na4Ti9O20 core-shell nanotubes for hybrid capacitive deionization with enhanced performance. *Desalination* 449, 69–77. doi: 10.1016/j.desal.2018.10.018

Yue, Z. S., Ma, Y. L., Zhang, J. W., and Li, H. (2019b). Pseudo-capacitive behavior induced dual-ion hybrid deionization system based on Ag@rGO parallel to Na1.1V3O7.9@rGO. *J. Mater. Chem. A* 7, 16892–16901. doi: 10.1039/C9TA03570B

Zhang, L., Liu, W. X., Shi, W. H., Xu, X. L., Mao, J., Li, P., et al. (2018). Boosting lithium storage properties of MOF derivatives through a wet-spinning assembled fiber strategy. *Chem. Eur. J.* 24, 13792–13799. doi: 10.1002/chem.201802826

Zhang, Q., Liao, C. Y., Zhai, T. Y., and Li, H. Q. (2016). A high rate 1.2V aqueous sodium-ion battery based on all NASICON structured NaTi2(PO4)3 and Na3V2(PO4)3. *Electrochim. Acta* 196, 470–478. doi: 10.1016/j.electacta.2016.03.007

Zhang, Q. C., Man, P., He, B., Li, C. W., Li, Q. L., Pan, Z. H., et al. (2020). Binder-free NaTi2(PO4)3 anodes for high-performance coaxial-fiber aqueous rechargeable sodium-ion batteries. *Nano Energy* 67:8. doi: 10.1016/j.nanoen.2019.104212

Zhang, X., Wang, X. G., Xie, Z. J., and Zhou, Z. (2016). Recent progress in rechargeable alkali metal-air batteries. *Green Energy Environ.* 1, 4–17. doi: 10.1016/j.gee.2016.04.004

Zhang, Y., Xia, X. H., Liu, B., Deng, S. J., Xie, D., Liu, Q., et al. (2019). Multiscale graphene-based materials for applications in sodium ion batteries. *Adv. Energy Mater.* 9:35. doi: 10.1002/aenm.201803342

Zhao, H. W., Chen, X. J., Wang, G. Z., Qiu, Y. F., and Guo, L. (2019). Two-dimensional amorphous nanomaterials: synthesis and applications. *2D Mater.* 6:28. doi: 10.1088/2053-1583/ab1169

Zhao, W. Y., Ding, M., Guo, L., and Yang, H. Y. (2019). Dual-ion electrochemical deionization system with binder-free aerogel electrodes. *Small* 15:8. doi: 10.1002/smll.201805505

Zhao, W. Y., Guo, L., Ding, M., Huang, Y. X., and Yang, H. Y. (2018). Ultrahigh-desalination-capacity dual-ion electrochemical deionization device based on $Na_3V_2(PO_4)_3$@C-AgCl electrodes. *ACS Appl. Mater. Interfaces* 10, 40540–40548. doi: 10.1021/acsami.8b14014

Zhao, Y. B., Liang, B. L., Wei, X. J., Li, K. X., Lv, C. C., and Zhao, Y. (2019). A core-shell heterostructured CuFe@NiFe Prussian blue analogue as a novel electrode material for high-capacity and stable capacitive deionization. *J. Mater. Chem. A* 7, 10464–10474. doi: 10.1039/C8TA12433G

Zhou, F., Gao, T., Luo, M., and Li, H. B. (2018). Heterostructured graphene@$Na_4Ti_9O_{20}$ nanotubes for asymmetrical capacitive deionization with ultrahigh desalination capacity. *Chem. Eng. J.* 343, 8–15. doi: 10.1016/j.cej.2018.02.124

Zhu, K., Zhang, H. Y., Ye, K., Zhao, W. B., Yan, J., Cheng, K., et al. (2017). Two-dimensional titanium carbide MXene as a capacitor-type electrode for rechargeable aqueous Li-ion and Na-ion capacitor batteries. *ChemElectroChem* 4, 3018–3025. doi: 10.1002/celc.201700523

Zubi, G., Dufo-Lopez, R., Carvalho, M., and Pasaoglu, G. (2018). The lithium-ion battery: state of the art and future perspectives. *Renew. Sust. Energy Rev.* 89, 292–308. doi: 10.1016/j.rser.2018.03.002

**Conflict of Interest:** The authors declare that the research was conducted in the absence of any commercial or financial relationships that could be construed as a potential conflict of interest.